Ranta, Mikaela; Hinkkanen, Marko; Dlala, Emad; Repo, Anna-Kaisa; Luomi, Jorma

Inclusion of hysteresis and eddy current losses in dynamic induction machine models

Published in:
IEEE International Electric Machines and Drives Conference (IEMDC'09)

DOI:
10.1109/IEMDC.2009.5075384

Published: 03/05/2009

Document Version
Peer-reviewed accepted author manuscript, also known as Final accepted manuscript or Post-print

Inclusion of Hysteresis and Eddy Current Losses in Dynamic Induction Machine Models

Mikaela Ranta, Marko Hinkkanen, Emad Dlala, Anna-Kaisa Repo, and Jorma Luomi
Department of Electrical Engineering
Helsinki University of Technology
Finland

***Abstract*—This paper proposes a method for including both hysteresis losses and eddy current losses in the dynamic space vector model of induction machines. The losses caused by the rotation and magnitude changes of the flux vector are taken into account. The model can be applied, for example, to time-domain simulations and real-time applications such as drive control. Finite element analysis, simulations, and laboratory experiments of a 45-kW motor are used for the investigation. It is shown that the model can predict the iron losses in a wide frequency range. The accuracy is significantly improved as compared to earlier models.**

I. Introduction

The control of induction machines in an electric drive is commonly based on a simplified circuit model that can represent the machine behavior. Depending on the degree of accuracy required from the model, various phenomena can be considered or omitted. For instance, incorporating iron losses into the model topology enhances the accuracy of the identified parameters and, therefore, the control of the motor [1]. Iron losses should also be taken into account in simulation models used in research and development of new control strategies, such as loss minimization control.

In a real electrical machine, the iron losses are caused by the magnetic field variation inside the magnetic materials as the slotting and the motion of the rotor create complicated magnetic flux patterns, even when the motor is fed by a sinusoidal supply. The frequency converter, however, aggravates the problem by increasing the harmonic content in the magnetic flux density and current density. Thus, the development of adequate methods for the loss prediction is difficult and requires in-depth treatment.

The losses are conceptually separated into two loss components, known as the hysteresis and eddy-current losses. The hysteresis losses are proportional to the frequency while the eddy current losses are proportional to the square of the frequency. Within the circuit model, the complexity is usually reduced. It is assumed that the iron losses simply depend on the flux linkages. Conventionally, the iron losses are modeled using a constant resistor placed in parallel with the magnetizing inductance, which corresponds to losses that are proportional to the square of the frequency [2]. Hence, the frequency dependency corresponds to that of the eddy current losses. In [3], the hysteresis losses are modeled by a nonlinear resistor depending on the instantaneous angular frequency of the stator flux. The model can predict the hysteresis losses if the magnitude of the flux vector is constant, but it fails to predict the losses caused by the pulsating flux magnitude.

In converter-fed induction machines, the dependency of the iron losses on the frequency and flux linkage amplitude is particularly important for the model of the machine. In this paper, the idea of a dynamic hysteresis model [4], [5] is used in the modeling of the iron losses. An explicit resistance function that includes the rotation and pulsation of the flux vector in the circuit model is proposed. Both hysteresis and eddy-current losses are modeled. The model is validated using finite element analysis, laboratory experiments, and simulations.

II. Preliminaries: Nonlinear Inductor

Before looking into induction machine models, modeling the iron losses of a nonlinear inductor is briefly described. A general framework for hysteresis modeling was presented in [4], [5] while no explicit functions were given. Here, an explicit function for the iron-loss resistance is proposed based on the desired steady-state iron-loss profile. In Section III, a similar approach will be used for modeling the iron losses in the induction machine.

A. Steady-State Model

The iron losses are typically modeled as

$$P_{\mathrm{Fe}} = k_{\mathrm{Ft}}\omega^2\Psi^2 + k_{\mathrm{Hy}}\omega\Psi^n \tag{1}$$

where the first term corresponds to the eddy-current losses and the second term corresponds to the hysteresis losses [6]. Ψ is the rms flux linkage and ω is the angular frequency. The exponent n in the hysteresis-loss term is typically $1\ldots2$. The coefficients k_{Ft} and k_{Hy} determine the ratio between the loss components. This steady-state model cannot be used in time-domain simulations since the angular frequency ω is irrelevant in transients and in the case of non-sinusoidal waveforms. However, the model will serve as a reference in the following when considering steady-state losses.

B. Dynamic Model

A hysteresis loop of a nonlinear saturable inductor can be modeled using a parallel nonlinear resistor as depicted in Fig. 1 [4], [5]. The terminal current is given as

$$\begin{aligned} i &= i' + i_{\mathrm{Fe}} \\ &= \frac{\psi}{L(\psi)} + \frac{u}{R(u,\psi)} \end{aligned} \tag{2}$$

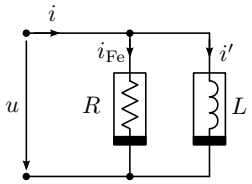

Fig. 1. Nonlinear inductor exhibiting a hysteresis loop.

where ψ is the instantaneous flux linkage, $u = \mathrm{d}\psi/\mathrm{d}t$ is the voltage across the inductor, L is a nonlinear inductance function, and R is a nonlinear iron-loss resistance function. The magnetic saturation can be modeled using the function [7]

$$L(\psi) = \frac{L_{\mathrm{u}}}{1 + \alpha|\psi|^a} \tag{3}$$

where L_{u} is the unsaturated inductance, and α and a are nonnegative constants.

The proposed iron-loss resistance function is

$$R(u, \psi) = \frac{R_{\mathrm{Ft}}}{1 + k|\psi|^{n-1}/|u|} \tag{4}$$

where R_{Ft} is a positive constant and k is a nonnegative constant.[1] The resistance function R can be interpreted as a parallel connection of two resistances: the constant resistance R_{Ft} related to the eddy-current losses and the voltage- and flux-dependent nonlinear resistance

$$R_{\mathrm{Hy}}(u, \psi) = \frac{R_{\mathrm{Ft}}}{k} \frac{|u|}{|\psi|^{n-1}} \tag{5}$$

related to the hysteresis losses.

The resistance function (4) leads to the instantaneous losses

$$p_{\mathrm{Fe}} = \frac{u^2 + k|\psi|^{n-1}|u|}{R_{\mathrm{Ft}}} \tag{6}$$

Assuming sinusoidally varying flux linkage, the average losses in steady state can be expressed as

$$P_{\mathrm{Fe}} = \frac{\omega^2\Psi^2 + k\omega\Psi^n}{R_{\mathrm{Ft}}} \tag{7}$$

i.e. they correspond to (1). The parameter k determines the ratio between the eddy-current and hysteresis losses. Selecting $n = 2$ leads to the quadratic dependency on the flux in both loss components. In this case, the eddy-current losses are equal to the hysteresis losses at the angular frequency $\omega = k$.

Examples of hysteresis loops, simulated using (2)–(4), are shown in Fig. 2. A sinusoidal voltage (or flux linkage) excitation was used in the case of Fig. 2(a). In the case of Fig. 2(b), the excitation voltage included a tenth-harmonic component; it can be seen that the model can produce minor hysteresis loops.

[1]In accordance with [8], R can be classified as a first-order nonlinear resistor.

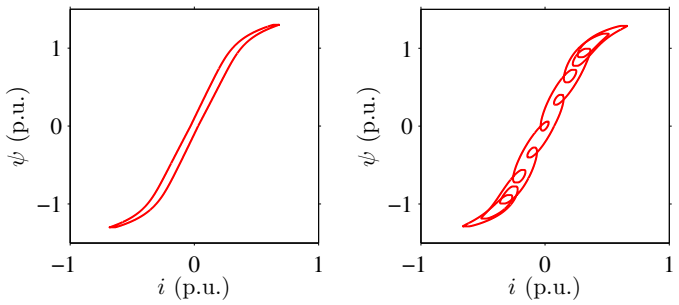

Fig. 2. Simulated hysteresis loops of a nonlinear inductor: (a) sinusoidal voltage exitation; (b) voltage excitation including a tenth-harmonic component. Parameter values are: $R_{\mathrm{Ft}} = 206$ p.u., $k = 3.05$ p.u., $n = 1.98$, $L_{\mathrm{u}} = 3.17$ p.u., $\alpha = 0.085$ p.u., and $a = 7.5$.

III. Γ Model of an Induction Machine

A. Voltage and Flux Equations

Fig. 3 shows the dynamic Γ model [2] of the induction machine in a coordinate system rotating at an arbitrary angular speed ω_{s}. Real-valued space vectors are used; for example, the stator flux vector is $\boldsymbol{\psi}_{\mathrm{s}} = [\psi_{\mathrm{sd}}, \psi_{\mathrm{sq}}]^{\mathrm{T}}$ and its magnitude is

$$\psi_{\mathrm{s}} = \sqrt{\psi_{\mathrm{sd}}^2 + \psi_{\mathrm{sq}}^2} \tag{8}$$

The orthogonal rotation matrix is

$$\mathbf{J} = \begin{bmatrix} 0 & -1 \\ 1 & 0 \end{bmatrix} \tag{9}$$

The induction machine model can be described by the voltage equations

$$\frac{\mathrm{d}\boldsymbol{\psi}_{\mathrm{s}}}{\mathrm{d}t} = \boldsymbol{u}_{\mathrm{s}} - R_{\mathrm{s}}\boldsymbol{i}_{\mathrm{s}} - \omega_{\mathrm{s}}\mathbf{J}\boldsymbol{\psi}_{\mathrm{s}} \tag{10a}$$

$$\frac{\mathrm{d}\boldsymbol{\psi}_{\mathrm{R}}}{\mathrm{d}t} = \boldsymbol{u}_{\mathrm{R}} - R_{\mathrm{R}}\boldsymbol{i}_{\mathrm{R}} - \omega_{\mathrm{r}}\mathbf{J}\boldsymbol{\psi}_{\mathrm{R}} \tag{10b}$$

where the stator voltage vector is denoted by $\boldsymbol{u}_{\mathrm{s}}$, the stator current vector by $\boldsymbol{i}_{\mathrm{s}}$, and the stator resistance by R_{s}. The rotor voltage vector is $\boldsymbol{u}_{\mathrm{R}}$ ($\boldsymbol{u}_{\mathrm{R}} = 0$ in cage-induction machines), the rotor current vector $\boldsymbol{i}_{\mathrm{R}}$, and the rotor resistance R_{R}. The angular slip frequency $\omega_{\mathrm{r}} = \omega_{\mathrm{s}} - \omega_{\mathrm{m}}$, where ω_{m} is the electrical angular speed of the rotor. The stator and rotor flux linkages are given by

$$\boldsymbol{\psi}_{\mathrm{s}} = L_{\mathrm{M}}(\boldsymbol{i}'_{\mathrm{s}} + \boldsymbol{i}_{\mathrm{R}}) \tag{11a}$$

$$\boldsymbol{\psi}_{\mathrm{R}} = \boldsymbol{\psi}_{\mathrm{s}} + L_{\sigma}\boldsymbol{i}_{\mathrm{R}} \tag{11b}$$

respectively, where $\boldsymbol{i}'_{\mathrm{s}} = \boldsymbol{i}_{\mathrm{s}} - \boldsymbol{i}_{\mathrm{Fe}}$, the magnetizing inductance is L_{M}, and the leakage inductance is L_{σ}. The iron loss current is

$$\boldsymbol{i}_{\mathrm{Fe}} = \frac{\boldsymbol{u}_{\mathrm{s}} - R_{\mathrm{s}}\boldsymbol{i}_{\mathrm{s}}}{R_{\mathrm{Fe}}} \tag{12}$$

where R_{Fe} is the iron-loss resistance. The magnetizing current is $\boldsymbol{i}_{\mathrm{M}} = \boldsymbol{i}'_{\mathrm{s}} + \boldsymbol{i}_{\mathrm{R}}$, and the leakage flux is $\boldsymbol{\psi}_{\sigma} = L_{\sigma}\boldsymbol{i}_{\mathrm{R}}$.

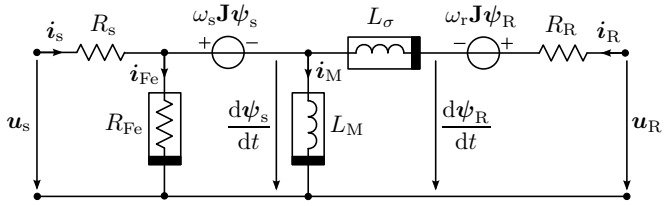

Fig. 3. Γ model in synchronous coordinates, where $\omega_\mathrm{r} = \omega_\mathrm{s} - \omega_\mathrm{m}$.

B. Power Balance

For per-unit quantities, the power balance of the induction machine model is given by

$$\boldsymbol{i}_\mathrm{s}^\mathrm{T}\boldsymbol{u}_\mathrm{s} + \boldsymbol{i}_\mathrm{R}^\mathrm{T}\boldsymbol{u}_\mathrm{R} = R_\mathrm{s}i_\mathrm{s}^2 + R_\mathrm{R}i_\mathrm{R}^2 + p_\mathrm{Fe} + \frac{\mathrm{d}W_\mathrm{f}}{\mathrm{d}t} + T_\mathrm{e}\omega_\mathrm{m} \quad (13)$$

where p_Fe represents the iron losses. The electromagnetic torque is

$$T_\mathrm{e} = \boldsymbol{i}_\mathrm{s}'^\mathrm{T}\mathbf{J}\boldsymbol{\psi}_\mathrm{s} = \boldsymbol{\psi}_\mathrm{R}^\mathrm{T}\mathbf{J}\boldsymbol{i}_\mathrm{R} \quad (14)$$

and the rate of change of the magnetic energy is

$$\begin{aligned}\frac{\mathrm{d}W_\mathrm{f}}{\mathrm{d}t} &= \boldsymbol{i}_\mathrm{s}'^\mathrm{T}\frac{\mathrm{d}\boldsymbol{\psi}_\mathrm{s}}{\mathrm{d}t} + \boldsymbol{i}_\mathrm{R}^\mathrm{T}\frac{\mathrm{d}\boldsymbol{\psi}_\mathrm{R}}{\mathrm{d}t} \\ &= i_\mathrm{M}\frac{\mathrm{d}\psi_\mathrm{s}}{\mathrm{d}t} + i_\mathrm{R}\frac{\mathrm{d}\psi_\sigma}{\mathrm{d}t}\end{aligned} \quad (15)$$

The last form is obtained by assuming the two flux vectors to be parallel with the corresponding current vectors in accordance with Fig. 3, while the inductances may be functions of the currents or fluxes. The magnetizing inductance L_M and the leakage inductance L_σ are assumed to be saturable but lossless. Hence, the incremental inductances should fulfill the reciprocity condition [9], [10]:

$$\frac{\partial\psi_\mathrm{s}}{\partial i_\mathrm{R}} = \frac{\partial\psi_\sigma}{\partial i_\mathrm{M}} \quad (16)$$

C. Magnetic Saturation

The magnetizing inductance saturates strongly as a function of the main flux (or the magnetizing current). Due to closed or skewed rotor slots, the magnetizing inductance may also saturate as a function of the leakage flux (or the rotor current). Similarly, the leakage inductance may saturate as a function of both the leakage flux and the main flux.

The saturation due to the main and leakage flux interaction can be modeled using the explicit inductance functions [11]

$$L_\mathrm{M}(\psi_\mathrm{s}, \psi_\sigma) = \frac{L_\mathrm{Mu}}{1 + \alpha\psi_\mathrm{s}^a + \frac{\gamma L_\mathrm{Mu}}{d+2}\psi_\mathrm{s}^c\psi_\sigma^{d+2}} \quad (17a)$$

$$L_\sigma(\psi_\mathrm{s}, \psi_\sigma) = \frac{L_{\sigma\mathrm{u}}}{1 + \beta\psi_\sigma^b + \frac{\gamma L_{\sigma\mathrm{u}}}{c+2}\psi_\mathrm{s}^{c+2}\psi_\sigma^d} \quad (17b)$$

where L_Mu and $L_{\sigma\mathrm{u}}$ are the unsaturated inductances. The parameters α, β, and γ as well as a, b, c, and d are nonnegative constants. It can be shown that the functions (17) fulfill the reciprocity condition (16). If the interaction between the main and leakage fluxes is insignificant, $\gamma = 0$ can be selected, resulting in the functions proposed in [7].

When the saturation is to be modeled, it is usually convenient to choose the stator flux vector and the rotor flux vector as state variables of the dynamic model, in order to avoid the differentiation of the inductance functions. An advantage from an implementation point of view is that the functions in (17) depend only on the state variables of the Γ model, i.e. on $\psi_\mathrm{s} = \|\boldsymbol{\psi}_\mathrm{s}\|$ and $\psi_\sigma = \|\boldsymbol{\psi}_\mathrm{R} - \boldsymbol{\psi}_\mathrm{s}\|$. Therefore, the augmentation of the Γ model with (17) does not involve algebraic loops.

D. Proposed Iron Loss Model

The stator iron losses of the induction machine are modeled by a nonlinear resistance R_Fe parallel to the magnetizing branch. An iron-loss resistance function corresponding to (4) is considered:

$$R_\mathrm{Fe}(u, \psi_\mathrm{s}) = \frac{R_\mathrm{Ft}}{1 + k\psi_\mathrm{s}^{n-1}/u} \quad (18)$$

where the voltage across the iron-loss resistance is

$$u = \|\boldsymbol{u}_\mathrm{s} - R_\mathrm{s}\boldsymbol{i}_\mathrm{s}\| \quad (19)$$

The voltage can also be expressed as

$$u = \left\|\frac{\mathrm{d}\boldsymbol{\psi}_\mathrm{s}}{\mathrm{d}t} + \omega_\mathrm{s}\mathbf{J}\boldsymbol{\psi}_\mathrm{s}\right\| \quad (20)$$

It can be seen that the voltage can describe both the changes in the flux amplitude and the rotation of the flux vector. As the resistance function is dependent on u, both rotational and alternating losses can be included in the model.

The resistance function leads to the iron losses

$$\begin{aligned}p_\mathrm{Fe} &= p_\mathrm{Ft} + p_\mathrm{Hy} \\ &= \frac{u^2}{R_\mathrm{Ft}} + \frac{k\psi_\mathrm{s}^{n-1}u}{R_\mathrm{Ft}}\end{aligned} \quad (21)$$

where p_Ft denotes the eddy current losses and p_Hy the hysteresis losses. The steady-state losses can be expressed as

$$P_\mathrm{Fe} = \frac{\omega_\mathrm{s}^2\psi_\mathrm{s}^2 + k|\omega_\mathrm{s}|\psi_\mathrm{s}^n}{R_\mathrm{Ft}} \quad (22)$$

for constant magnitude ψ_s and constant angular frequency ω_s of the flux.

E. Implementation

The iron loss resistance in (18) depends on the stator current via the voltage u in (19). In a voltage-driven dynamic model using the fluxes as state variables, the currents $\boldsymbol{i}_\mathrm{s}'$ and $\boldsymbol{i}_\mathrm{R}$ can be evaluated from the flux equations (11), whereas the stator current $\boldsymbol{i}_\mathrm{s}$ is unknown. To avoid algebraic loops in the implementation, the dependency of R_Fe on the stator current can be removed by algebraic manipulation. Since $\boldsymbol{i}_\mathrm{s} = \boldsymbol{i}_\mathrm{s}' + \boldsymbol{i}_\mathrm{Fe}$, the iron-loss current can be expressed using $\boldsymbol{i}_\mathrm{s}'$ as

$$\boldsymbol{i}_\mathrm{Fe} = \frac{\boldsymbol{u}_\mathrm{s} - R_\mathrm{s}\boldsymbol{i}_\mathrm{s}'}{R_\mathrm{Fe}'} \quad (23)$$

where the modified resistance function is

$$\begin{aligned}R_\mathrm{Fe}'(u', \psi_\mathrm{s}) &= R_\mathrm{s} + R_\mathrm{Fe} \\ &= \frac{R_\mathrm{s} + R_\mathrm{Ft}}{1 + k\psi_\mathrm{s}^n/u'}\end{aligned} \quad (24)$$

The voltage $u' = \|\boldsymbol{u}_\mathrm{s} - R_\mathrm{s}\boldsymbol{i}_\mathrm{s}'\|$ now depends on $\boldsymbol{i}_\mathrm{s}'$.

IV. Results

The iron loss model was investigated by means of finite element analysis, laboratory experiments, and time domain simulations. A 45-kW cage-induction machine was used in these investigations. The rating of the machine is: voltage 400 V; current 81 A; frequency 50 Hz; speed 1477 r/min; and torque 291 Nm.

A. Finite Element Analysis

To identify the proposed iron loss model, finite element analysis (FEA) was applied to the no-load operation at various frequencies. In the computations, the stator winding was supplied with a balanced three-phase voltage system. Three different voltage levels were applied at each frequency. In the two-dimensional, time-stepping FEA, a magnetodynamic vector hysteresis model and the classical eddy-current loss model were used for taking the iron loss components into account [12], [13]. The iron loss model in (22) was fitted to the iron losses obtained from the FEA. The least-squares curve fitting algorithm *lsqnonlin* provided by Matlab was used for the data fitting. The parameter values $R_{\mathrm{Ft}} = 249$ p.u., $k = 0.992$ p.u., and $n = 1.520$ were obtained.

In Fig. 4, the iron losses obtained from FEA and the fitted iron losses are shown. The iron losses at frequencies up to 50 Hz are shown in Fig. 4(a). The solid lines show the behavior of the losses of the fitted model at the constant stator flux levels 0.37 p.u., 0.74 p.u. and 0.81 p.u. In the field weakening region above 50 Hz, the flux was inversely proportional to the frequency. The data in this region are shown in Fig 4(b), where the solid lines correspond to constant voltage levels. It can be seen that the model fits well to the data obtained from the FEA in a wide frequency range. If the exponent n is fixed to 2, the sum of the iron loss square errors in the fitted model is five times that obtained from the proposed model. If a constant resistance is used, the square error is 68 times larger.

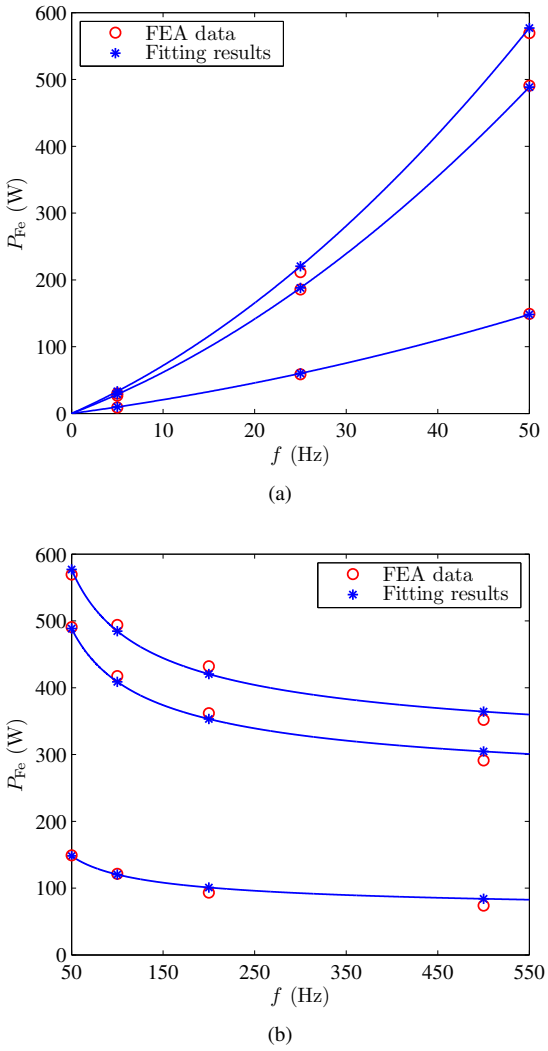

Fig. 4. (a) The iron losses obtained from FEA and the iron losses obtained from the fitted model up to 50 Hz. The iron losses of the fitted model at three constant flux levels are shown by solid lines. (b) The iron losses from FEA and the fitted iron losses used in the field weakening region. The solid lines correspond to constant voltage levels.

B. Experimental Results

In the laboratory experiments, the induction motor was fed by a frequency converter controlled by a dSPACE DS1104 PPC/DSP board. The slip was controlled by a servo motor coupled to the shaft of the induction machine. The stator voltage and the stator current were measured at different stator frequencies and stator flux levels under no-load operation. The stator flux amplitudes were 0.35 p.u., 0.5 p.u., 0.7 p.u. and 0.8 p.u. The fundamental-frequency components of the voltage and current were obtained from the measured signals by means of Fourier transformation. The total losses of the induction machine at the fundamental frequency could thus be calculated. The stator resistance was measured in advance by means of a DC test. At the synchronous speed, the total losses consist of the stator iron losses and the resistive losses of the stator winding. The stator iron losses at the fundamental frequency were thus obtained by subtracting the resistive losses from the total losses.

The iron loss model in (22) was fitted to the measured iron losses. The parameter values $R_{\mathrm{Ft}} = 206$ p.u., $k = 3.05$ p.u., and $n = 1.98$ were obtained. The measured iron losses and the iron losses obtained from the fitted model are shown in Fig. 5. The iron losses are slightly higher than those obtained from the FEA. According to the fitted model, the hysteresis losses dominate in the frequency range considered. At the rated stator frequency, the hysteresis losses constitute approximately 75% of the total losses.

For comparison, a model with a constant iron loss resistance was fitted to the measured data. This model leads to iron losses that are proportional to the square of the angular frequency, i.e. a frequency dependence corresponding to the eddy current losses. The value of the fitted resistance is 46.0 p.u. The results are illustrated in Fig. 6. It is obvious that a constant iron loss resistance cannot model the measured data well.

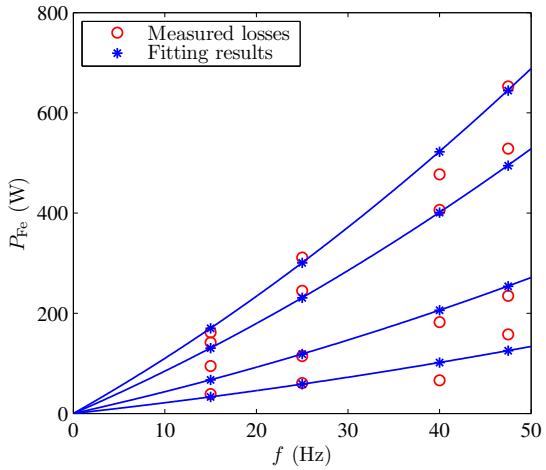

Fig. 5. The measured iron losses and the iron losses obtained from the fitted model. The solid lines show the iron losses obtained from the fitted model at constant flux levels.

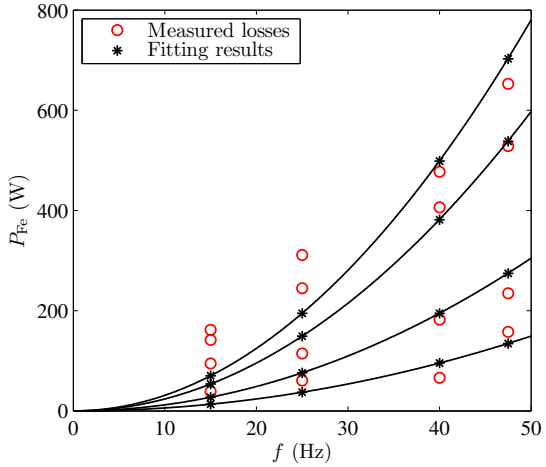

Fig. 6. The measured iron losses and the iron losses obtained from the fitted model as the iron-loss resistance is assumed to be constant. The solid lines show the iron losses obtained from the fitted model at constant flux levels.

C. Time-Domain Simulations

The proposed iron loss model was investigated by means of simulations in the Matlab/Simulink environment. The 45-kW induction machine was modeled using (10), (11), (17), (23), and (24). The parameter values obtained from the data fitting of the measured iron losses were used.

As an example, a DC voltage was applied to achieve the rated flux, and a 2-Hz sinusoidal voltage signal was superimposed on the DC voltage to produce pulsations in the flux amplitude. The amplitude of the sinusoidal voltage was 0.02 p.u. The iron loss components and the iron loss current are shown in Fig. 7. The iron losses mostly consist of the hysteresis losses, the eddy current losses being less than 1% of the total losses at the low frequency considered. In [3], a nonlinear resistor depending on the instantaneous angular frequency of the stator flux is used to model the iron losses.

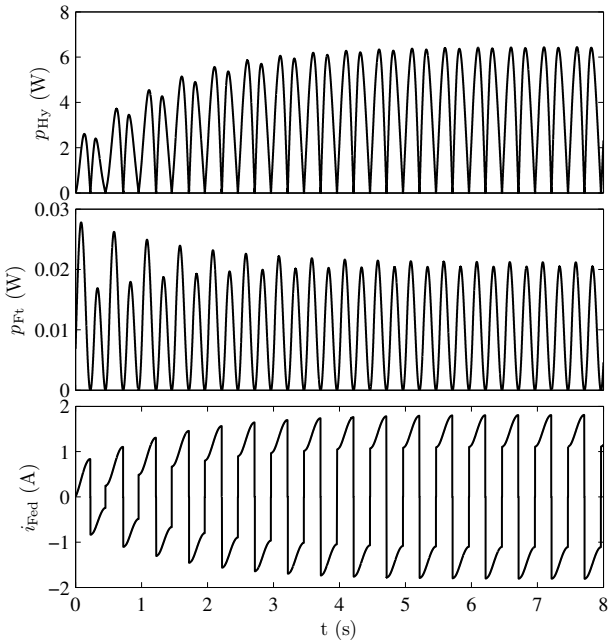

Fig. 7. The hysteresis losses, eddy current losses and the current through the iron loss resistance obtained from simulations; the motor is magnetized by a DC voltage, and a sinusoidal voltage is superimposed on the DC voltage to produce flux pulsations.

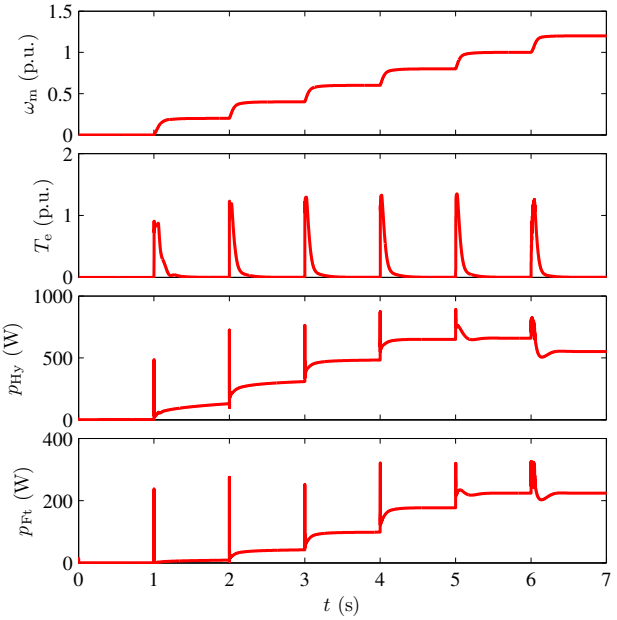

Fig. 8. Simulation results showing speed steps at no load. The first subplot shows the speed, the second subplot shows the electromagnetic torque, the third subplot shows the instantaneous hysteresis losses, and the last subplot shows the eddy current losses.

If this resistor would be used, the iron losses would be zero as the stator flux vector does not rotate.

The simulation results as rotor flux oriented vector control is applied are shown in Fig. 8. The speed reference is increased in steps of 0.2 p.u. and the load torque is zero. The inertia of the machine is 1.10 kgm^2. As the speed exceeds the rated value,

the hysteresis losses start to decrease as the flux amplitude decreases. The eddy current losses are approximately constant in the field weakening region.

V. Conclusions

In this paper, an iron loss model is proposed where both the hysteresis losses and the eddy current losses are modeled. The losses caused by the rotation of the flux vector as well as the losses caused by the pulsation of the flux vector magnitude are taken into account. A least-squares algorithm is used to fit the model to data from finite element analysis and laboratory experiments. It is shown that the model can predict the iron losses in a wide frequency range. Particularly at low frequencies, the accuracy is improved as compared to conventional models.

Acknowledgement

The authors gratefully acknowledge ABB Oy and the Academy of Finland for the financial support and Mr. Toni Tuovinen for the fitting of the inductance functions.

References

[1] E. Levi, M. Sokola, A. Boglietti, and M. Pastorelli, "Iron loss in rotor-flux-oriented induction machines: identification, assessment of detuning and compensation," *IEEE Trans. Power Electronics*, vol. 11, no. 5, pp. 698–709, Sept. 1996.

[2] G. R. Slemon, "Modelling of induction machines for electric drives," *IEEE Trans. Ind. Appl.*, vol. 25, no. 6, pp. 1126–1131, Nov./Dec. 1989.

[3] S. Shinnaka, "Proposition of new mathematical models with stator core loss factor for induction motor," *Electr. Eng. in Japan*, vol. 134, no. 1, pp. 64–75, 2001.

[4] L. O. Chua and K. A. Stromsmoe, "Lumped-circuit models for nonlinear inductors exhibiting hysteresis loops," *IEEE Trans. Circuit Theory*, vol. CT-17, no. 4, pp. 564–574, Nov. 1970.

[5] ——, "Mathematical model for dynamic hysteresis loops," *Int. J. Eng. Sci.*, vol. 9, no. 5, pp. 435–450, May 1971.

[6] D. W. Novotny, S. A. Nasar, B. Jeftenic, and D. Maly, "Frequency dependence of time harmonic losses in induction machines," in *Proc. ICEM'90*, vol. 1, Cambridge, MA, Aug. 1990, pp. 233–238.

[7] H. C. J. de Jong, "Saturation in electrical machines," in *Proc. ICEM'80*, vol. 3, Athens, Greece, Sept. 1980, pp. 1545–1552.

[8] L. O. Chua, "Device modeling via basic nonlinear circuit elements," *IEEE Trans. Circuits Syst.*, vol. CAS-27, no. 11, pp. 1014–1044, Nov. 1980.

[9] P. W. Sauer, "Constraints on saturation modeling in ac machines," *IEEE Trans. Energy Convers.*, vol. 7, no. 1, pp. 161–167, Mar. 1992.

[10] M. Hinkkanen, A.-K. Repo, M. Cederholm, and J. Luomi, "Small-signal modelling of saturated induction machines with closed or skewed rotor slots," in *Conf. Rec. IEEE-IAS Annu. Meeting*, New Orleans, LA, Sept. 2007, pp. 1200–1206.

[11] T. Tuovinen, M. Hinkkanen, and J. Luomi, "Modeling of mutual saturation in induction machines," in *Conf. Rec. IEEE-IAS Annu. Meeting*, Edmonton, Canada, Oct. 2008, CD-ROM.

[12] E. Dlala, "Magnetodynamic vector hysteresis models for steel laminations of rotating electrical machines," Ph.D. dissertation, Dep. Elect. Eng., Helsinki Univ. Tech., Espoo, Finland, April 2008.

[13] ——, "Comparison of models for estimating magnetic core losses in electrical machines using the finite-element method," *IEEE Trans. Magn.*, vol. 45, no. 2, pp. 716–725, Feb. 2009.